Stacking sequence constraints in non-conventional composite laminate optimisation

Peeters, DMJ; Abdalla, MM

DOI
10.2514/6.2016-1969

Publication date
2016

Document Version
Accepted author manuscript

Published in
Proceedings of the 57th AIAA/ASCE/AHS/ASC structures, structural dynamics, and materials conference

Stacking sequence constraints in non-conventional composite laminate optimisation

Daniël Peeters* and Mostafa Abdalla†

Delft University of Technology, 2629 HS Delft, The Netherlands

A method to take design guidelines into account during the optimisation of non-conventional laminates is developed. Non-conventional laminates are defined as laminates with angles other than 0°, ±45°or 90°. The optimisation is performed using the method of successive approximations. Some design guidelines are interpreted as a limit on angle or angle difference, and are implemented as such. The 10% rule is interpreted as a limit on the ratio of the stiffness in any two directions. It is posed in the optimisation as a positive-semi-definite matrix constraint. Other design guidelines are implemented as user-defined options, for example having a ±45°layer on the outside. Initial results of a square plate under bi-axial tension show that the constraints are always satisfied, while achieving good performance.

I. Introduction

Composite materials are often used in aerospace industry because of their high stiffness-to-weight and strength-to-weight ratios. Because the layers have different fibre orientations, the material properties can easily be tailored to the applied load. The percentage of composite material in aircraft has gradually increased since their first use in the 1970s.[1] Some modern aircraft, such as the B-787 and A-350, are made of over 50% composite material.[2,3]

The different fibre orientations are usually limited to 0°, ±45°, and 90°. This restriction comes from the early days of composite materials when hand lay-up was often used, and these angles could be laid down accurately. Since these fibre orientations have often been used, more test data is available, and engineers are more confident using them. Nowadays, sometimes multiples of 15°or 30°are used. Laminates with these restricted set of possible fibre angles will be referred to as *conventional laminates* (CL) in this paper.

Since conventional laminates are already in use for quite some time, design guidelines have been built up over time. Some of these guidelines are for manufacturing reasons, for example having a symmetric laminate. Others are to avoid preliminary failure under low unexpected load, for example the 10% rule. Yet another reason is based on experience with impact, for example having ±45°layers on the outside. Hence, by following these design guidelines, a lot of experience is taken into account.

During optimisation of conventional laminates, the design guidelines are usually taken into account. Because of the limited number of options, the most popular optimisation techniques are the direct search and heuristic techniques.[4] The simplest optimisation technique is enumeration, which is only feasible when the number of possibilities is limited.[5]

A less computational expensive method is the use of evolutionary search algorithms; the most popular of which are Genetic Algorithms (GA).[6–8] Other probabilistic search techniques are swarm techniques such as the ant colony optimisation, which was shown to have the same, or better, performance as GAs.[9] These direct search methods employ multiple design rules within the search algorithm. However, if the number of options increases, even if multiples of 15°are used, the efficiency of evolutionary algorithms already leads to long computational time.

With the rise of fibre placement machines, the limited set of possible fibre angles disappeared: using these machines, fibres can be laid down accurately in any direction. This increases the ability to tailor

*Ph.D. Student, Faculty of Aerospace Engineering, Aerospace Structures and Computational Mechanics, Kluyverweg 1; D.M.J.Peeters@tudelft.nl; Student member AIAA

†Associate Professor, Faculty of Aerospace Engineering, Aerospace Structures and Computational Mechanics, Kluyverweg 1; M.M.Abdalla@tudelft.nl

the properties of the composite material. Hence, the stiffness-to-weight and strength-to-weight ratios can increase even further. However, the possible fibre angles can now be multiples of 5°, or even smaller, making evolutionary algorithms a computationally very costly option.

Since every fibre angle can be laid down, the fibre angle can be seen as a continuous variable during optimisations. This means more computationally efficient methods such as gradient based methods can be used. Classical techniques such as the steepest descent or conjugate gradient method have been used for unconstrained optimisation; and sequential quadratic programming and the method of feasible directions for constrained problems.[4] To save computational time response approximation schemes are used. By combining the convex linearisation approximation of Fleury and Braibant[10] and the method of Conservative convex separable approximations proposed by Svanberg,[11] a good approximation scheme is available to calculate the gradient for a relatively low computational cost.[12]

This paper aims at interpreting design guidelines in such a way they can be posed as constraint in a gradient-based optimisation. A lot of design guidelines, such as the 10% rule, are based on counting the number of plies in a certain direction. When the fibre angle is continuous, enforcing these rules on a ply-count base will drastically decrease the design space of the optimisation. Hence, the guidelines have to be interpreted to be posed as a constraint during gradient-based optimisation. Posing the design guidelines as constraints will combine the experience on which these guidelines are based, with the possible advantages of different non-conventional laminates.

This paper starts by explaining in detail which non-conventional laminates are used in section II. Next, an overview of the design guidelines to be implemented is given in section III. Before diving into how these design guidelines are implemented, first the optimisation in which they will be embedded in discussed in section IV. Next the design guidelines are discussed in sections V to VII. Finally results are shown in section VIII, and the conclusions are given in section IX.

II. Non-conventional laminates

Conventional laminates are defined in this work as laminates currently used in industry. Most laminates are still limited to the set of 0°, ±45°, and 90°. Sometimes also multiples of 15°or 30°are used. Laminates with plies in another direction than these are considered to be non-conventional in this work. Using fibre placement machines fibres can be laid down accurately in any direction.

Next to the angles being possible in any direction, two other sorts of non-conventional laminates are considered. The first one are dispersed laminates where the fibre angles are spread out over all possible directions. The second are APPLY laminates, which means advanced placed ply, which mimics the behaviour of woven composites at a fast deposition rate. Both are discussed in more detail in the next two subsections.

A. Dispersed laminates

In nature it is observed that parts that have to withstand a lot of impacts, such as claws, have a helical arrangement of mineralised fibre layers.[13] This can be mimicked by placing the fibres also in a helical shape, as shown in Figure 1. Doing so has been shown to have a positive effect on post-impact behaviour. The helical shape improves the post impact behaviour, but the in-plane properties are quasi-isotropic this way, reducing the potential weight savings composites may lead to.

The good impact resistance is achieved by maximising the difference in fibre angles between consecutive plies. This reduces the interlaminar shear stress by potentiating crack fibre bridging and increasing the number of interfaces (i.e., compared to conventional laminates consecutive plies no longer have the same orientation). Hence, to improve post-impact behaviour dispersed laminates have a large change in ply angle between consecutive layers to improve impact resistance.[14] This has been shown to improve the post-impact behaviour of composites.[15,16] This will be implemented in the optimisation as a minimal change in fibre angle between consecutive plies.

B. APPLY concept

Interweaving of plies is another possible way to improve post-impact behaviour. By weaving the plies, delamination is stopped at the place where the weave is: the interface between the two angles where the delaminations occurred suddenly stops. Furthermore, interwoven plies can be seen as one thick layer, being

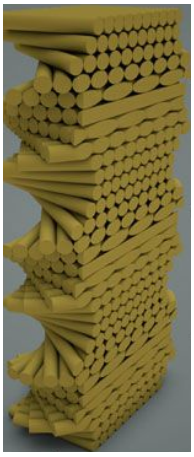

Figure 1. helical dispersing of plies[13]

stiff in two rather than one direction. Disadvantage is that interweaving plies is a time-consuming and expensive process.

The characteristics of woven plies can be obtained using the APPLY principle: when laying down 2 layers, first half of the fibres in one direction is laid down, always leaving a gap of exactly one bandwidth, next the fibres in the other direction are laid down, and the gaps are filled in step three and four. This is shown in Figure 2.[17] APPLY combines the advantages of the characteristics of woven plies with the fast and accurate manufacturing using fibre placement machines.

Interweaving plies is easiest if the difference between the plies is 90°, as shown in Figure 2. However, as long as a minimal difference between plies is adhered to, they can be interwoven using the APPLY principle. In this work it is assumed balanced pairs of +/- angles are interwoven. To make sure these can be interwoven, an upper and lower bound on fibre angles has to be implemented: directions too close to 0°or 90°have to be avoided.

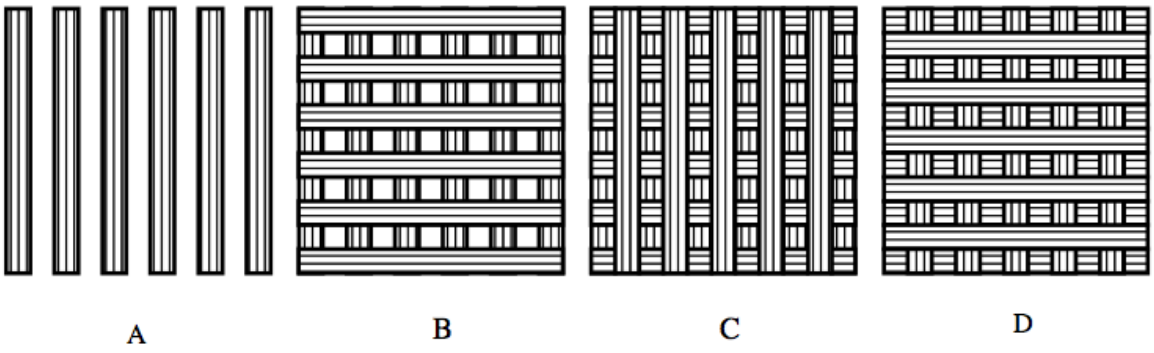

Figure 2. schematic overview of the manufacturing using the APPLY principle[17]

III. Design guidelines

As mentioned in the previous section, dispersed laminates and APPLY have their own limitations, for completeness they are repeated here:

1. For APPLY laminates each layer pair is balanced (i.e., in the form $\pm\theta$). An upper and lower bound on the ply angle is imposed to ensure manufacturability.

2. For dispersed laminates a lower bound on the difference between adjacent fibre angles is imposed.

Next, there are industrial guidelines currently implemented in conventional laminate design. The stacking sequence constraints are listed here based on the work by Beckwith and a NASA report:[18,19]

3. The ply contiguity rule, which enjoins the designer to avoid stacking too many plies, usually the limit is set to 4, with the same angle next to each other.

4. Minimise the difference between adjacent fibre angles. If this is not done, the chance of delaminations increases and residual stresses are more likely.

5. The 10 % rule, which states that 10 % of the plies has to be in 0°, 45°, 90°and -45°direction. This makes sure the laminate is not too anisotropic and has at least some resistance against longitudinal (0°), transverse (90°) and shear loading (± 45°). This will also reduce the free-edge stresses and avoid micro-cracking.

6. A laminate should be symmetric about its middle surface. This avoids extension-bending coupling, in other words: the B-matrix is zero.

7. The balance constraint which states that 45°layers should be added in pairs (i.e., with a -45°layer).

8. Put the 45 and -45°layer in contact with each other to minimise interlaminar shear.

9. Add a fabric layer to the inner or outer layer to improve impact damage resistance.

10. Add ±45°layers on outside. This improves the buckling resistance and has a better damage tolerance.

11. Maintain a homogeneous stacking sequence by banding several plies of the same orientation together.

12. keep a reasonable number or primary load-carrying plies away from the outer surfaces. This rule avoids impact damage on the outside to be critical for the primary load-carrying capability.

More guidelines, relating to thermal effects, bonded and bolted joints, exist, but since no thermal effects or joints are used in the current work, these guidelines are not mentioned here.

How the different guidelines are adhered to is described in the following sections. First, the limits on fibre angles, rules 1 - 4, are discussed in section V. Next, he implementation of the 10 % rule will be discussed in section VI. All remaining guidelines are discussed in section VII.

IV. Optimisation procedure

In structural optimisation, the minimisation of an objective response (e.g., weight or compliance) subject to performance constraints (e.g., on stresses or displacements) is studied. More generally, the worst case response, for example in the case of multiple load cases, is optimised. Additional constraints not related to structural responses may also be imposed to guarantee certain properties of the design such as manufacturability. The following general problem formulation is considered:

$$\begin{aligned} \min_{\boldsymbol{x}} \quad & \max_{n}(f_1, f_2, ..., f_n) \\ s.t. \quad & f_{n+1}, ..., f_m \leq 0 \\ & \boldsymbol{x}_i \in \mathcal{D}_i \end{aligned} \tag{1}$$

The functions f_i depend on the design variables; f_1 to f_n denote structural responses that are optimised and f_{n+1} to f_m denote structural responses that are constrained. The feasible region is denoted by $\mathcal{D}$. This problem will be solved using successive approximations: one starts from a certain fibre angle distribution, constructs the approximations based on the optimal stiffness distribution, optimises the approximations and updates the approximations based on the new fibre angles. The optimisation is performed using a predictor-corrector interior-point method. This is repeated until convergence is reached. Convergence is defined in this work by the change in objective function: if this is smaller than a certain threshold, usually 10^{-3} is used, the solution is assumed to be converged.

Structural responses, such as buckling loads, stiffness, and strength, are calculated using a finite element (FE) analysis. Since each FE analysis is computationally expensive, greater efficiency can be achieved by

using structural approximations to reduce the required number of FE analyses.[12,20] The exact FE response f is approximated in terms of the in- and out-of-plane stiffness matrices $\boldsymbol{A}$ and $\boldsymbol{D}$ and their reciprocals:[21]

$$f^{(1)} \approx \sum_{n=1}^{N} \boldsymbol{\phi}_m : \boldsymbol{A}^{-1} + \boldsymbol{\phi}_b : \boldsymbol{D}^{-1} + \boldsymbol{\psi}_m : \boldsymbol{A} + \boldsymbol{\psi}_b : \boldsymbol{D} + c \tag{2}$$

where the : operator represents the Frobenius inner product, $\boldsymbol{A} : \boldsymbol{B} = tr(\boldsymbol{A} \cdot \boldsymbol{B}^T)$; $\boldsymbol{\phi}$ and $\boldsymbol{\psi}$ are calculated from sensitivity analysis.[22,23] Subscripts m and b denote the membrane and bending parts respectively. This approximation is a generalisation of the linear-reciprocal approximations used in the convex linearisation method.[10] The approximations are convex functions in stiffness space provided that $\boldsymbol{\phi} \geq 0$, a condition that is always satisfied by construction.[?] The free term c equals zero for many types of responses that enjoy homogeneity properties.

In this work the fibre angles are the design variables. Seen as a function of the fibre angles, the level one approximation, eq. (2), no longer has a simple mathematical form and is not generally convex, hence, a level two approximation is constructed based on the level one approximation in terms of the fibre angles:

$$f^{(2)} \approx f_0^{(1)} + \boldsymbol{g} \cdot \Delta\boldsymbol{\theta} + \Delta\boldsymbol{\theta}^T \cdot \boldsymbol{H} \cdot \Delta\boldsymbol{\theta} \tag{3}$$

where $f_0^{(1)}$ denotes the value, $\boldsymbol{g}$ the gradient and $\boldsymbol{H}$ the Gauss-Newton part of the Hessian of the level one approximation at the approximation point.[12]

To achieve global convergence, every iteration has to be an improvement step, meaning the constraints have to be satisfied and the objective function is improved. To achieve this, a damping function is added to the level two approximation, consisting of the damping function d_1, and a damping factor ρ_1 that is changed during the optimisation. The total approximation thus becomes:

$$f_\theta \approx f^{(2)} + \rho_1 \cdot d_1(\theta) \tag{4}$$

The details on the fibre angle optimisation, the interior-point method used, and the damping function used can be found in Peeters et al.[12]

V. Limits on angles

Two different limits for angles exist: the limits on the angle, and the limits on the difference between adjacent angles. For the limits on the fibre angle, both the minimal and maximal is due to the APPLY principle, rule 1. A minimal change between consecutive plies exists due to the dispersed laminates possibility, rule 2. The maximum number of plies with the same orientation, rule 3, is also enforced using a minimal change in fibre angle: the maximum number of plies with the same orientation is assumed to be one. The final rule implying a limit on the change in fibre angles is rule 4, which states that the change in fibre angles should be minimal: this is implemented as a maximal change in fibre angles.

Since all limits (minimal and maximal angle and angle difference) look quite similar, only the maximum difference between adjacent plies will be derived in this section. For the other three limits, the constraint and way to implement it in the optimisation will be shown without derivation.

The physical reason for the maximum difference between two adjacent plies are interlaminar stresses occurring. These arise due to the mismatch in stiffness between the plies with different orientation. According to Herakovich,[24] the two most important properties are the Poisson's ratio ν and the coefficient of mutual influence η, defined as

$$\nu_{xy} = \frac{-\epsilon_y}{\epsilon_x} = \frac{a_{12}}{a_{11}} \tag{5}$$

$$\eta_{xy,_x} = \frac{\gamma_{xy}}{\epsilon_y} = \frac{a_{16}}{a_{11}} \tag{6}$$

where $\boldsymbol{a}$ is the inverse of the in-plane stiffness matrix $\boldsymbol{A}$.

The code is verified by creating the plots showing ν and η as a function of the fibre angle. For this verification the following material data were used: $E_1 = 181$GPa, $E_2 = 11.3$GPa, $G_{12} = 7.17$GPa and $\nu_{12} = 0.28$. The plots are shown in Figure 3. These curves look the same as the ones shown by Herakovich,[24] and have the maximum at the same location. Hence, the code can be assumed to be verified.

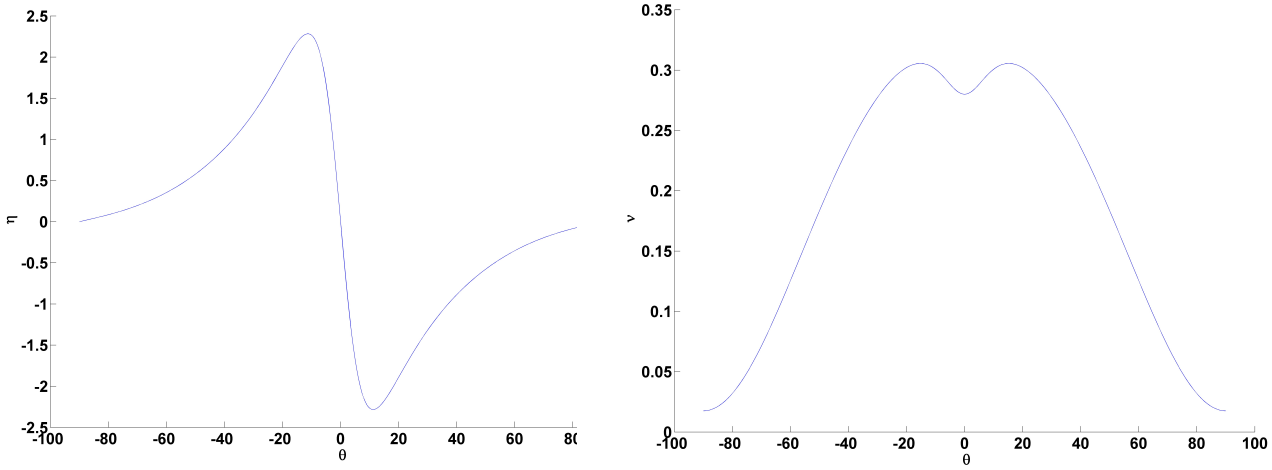

(a) η **(b)** ν

Figure 3. ν **and** η **as a function of the fibre angle**

The difference in ν and η as a function of the difference in angles is the critical factor for interlaminar stresses. The difference in fibre angles, for different average angles, is plotted in Figure 4, with a $\sin(\theta)^2$ plotted on top. The difference in η is clearly very large for small differences, hence it will not be taken into account further: it would be too restrictive. Looking at the difference in ν, it can be seen that the $\sin(\theta)^2$ matches the shape quite well. It also captures the periodicity of the difference in Poisson's ratio. To limit the interlaminar stresses, the constraint will be of the form $\sin(\theta_k - \theta_{k+1})^2 \leq \sin(\Delta\theta_{max})^2$ where k and k+1 denote the layer of the laminate, and θ_{max} is user-defined, based on the material used.

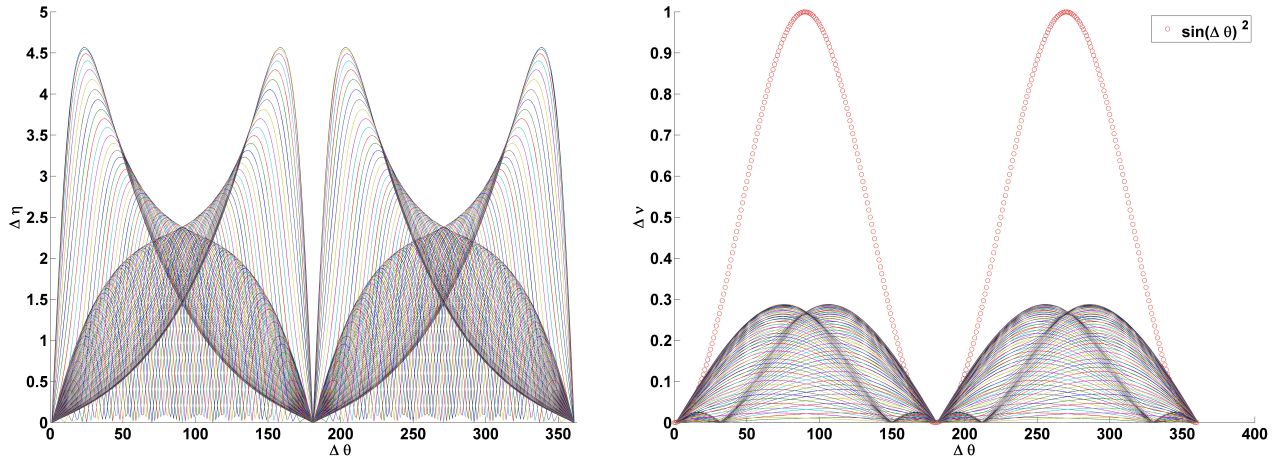

(a) $\Delta\eta$ **(b)** $\Delta\nu$

Figure 4. difference in ν **and** η **as a function of the change in fibre angle**

The optimisation problem, with only the maximal angle difference constraint is formulated as:

$$\min_{\boldsymbol{x}} \quad f \tag{7}$$

$$s.t. \quad sin\left(\theta_k - \theta_{k+1}\right)^2 \leq M \quad k = 1, ..., l-1 \tag{8}$$

where M denotes the squared of the sine of the maximal angle difference, and l the total number of layers.

A slack variable and a damping function are added:

$$\min_{\boldsymbol{x}} \quad f + \rho_1 d_1(x) \tag{9}$$

$$s.t. \quad sin\left(\theta_k - \theta_{k+1}\right)^2 - M + \rho_3 \cdot d_{(3k)}(x) + s_{d_k} = 0 \quad k = 1, ..., l-1 \tag{10}$$

$$s_d \geq 0 \tag{11}$$

The damping function is defined as:

$$d_3 = \frac{\left(\Delta\theta_k - \Delta\theta_{k+1}\right)^2}{2} \tag{12}$$

The Lagrangian can be written as:

$$\mathcal{L} = f + \rho_1 d_1(x) + \sum_k \lambda_k \cdot \left(sin\left(\theta_k - \theta_{k+1}\right)^2 - M + \rho_3 d_{(3k)}(x) + s_{d_k}\right) + \mu \cdot ln(s_{d_k}) \tag{13}$$

The solution procedure is explained in Appendix A.

VI. 10 % rule

Implementing the 10% rule as stated in section III, is not easy in the context of NCL design. When using a limited set of fibre angles, having a minimum number of layers in each direction can be relatively easy enforced. However, in the current optimisation, the fibre angle is seen as a continuous variable, making it hard to enforce angles of exactly 0°, 90°and ±45°in the optimisation. Furthermore, the 10% rule prescribes at least 40 % of the layers, considerably limiting the design space.

The 10% rule has previously been interpreted by Abdalla et al. as a robustness rule: a minimum stiffness has to be achieved in all directions.[25] This interpretation has been used to replace the ply count-based rule even in the context of CL.[26] The big advantage of this interpretation is that it is continuous. A disadvantage of this stiffness-formulation is the loss of dispersion of the plies, which can be (partly) counter-acted by a minimum change in fibre angle between consecutive plies.

According to Abdalla et al.,[25] the 10% rule can be written as a constraint on the minimum eigenvalue of the problem:[25]

$$\boldsymbol{A} : \epsilon = \gamma \bar{\boldsymbol{A}} : \epsilon \tag{14}$$

where ϵ is the in-plane eigen-strain vector; $\bar{\boldsymbol{A}}$ is the quasi-isotropic A-matrix of an arbitrary in-plane stiffness matrix $\boldsymbol{A}$, defined as:

$$\bar{\boldsymbol{A}} = \begin{bmatrix} \bar{A}_{11} & \bar{A}_{12} & 0 \\ \bar{A}_{12} & \bar{A}_{11} & 0 \\ 0 & 0 & \bar{A}_{66} \end{bmatrix} \tag{15}$$

with

$$\bar{A}_{11} = \frac{3A_{11} + 3A_{22} + 2A_{12} + 4A_{66}}{8} \tag{16}$$

$$\bar{A}_{12} = \frac{A_{11} + A_{22} + 6A_{12} - 4A_{66}}{8} \tag{17}$$

$$\bar{A}_{66} = \frac{A_{11} + A_{22} - 2A_{12} + 4A_{66}}{8} \tag{18}$$

The degree of isotropy of the laminate is given by the minimum eigenvalue γ_{min}: the laminate is considered robust if

$$\gamma_{min} \geq \alpha \tag{19}$$

The lower bound on α is dependent of the minimum percentage in ply count p:

$$1 - \alpha = \frac{5}{6}\left(1 - 4p\right) \tag{20}$$

for the traditional 10% rule $p = 0.1$ and $\alpha = 0.5$.

The eigenvalue constraint can be rewritten as a semi-definite matrix constraint:

$$\left(\boldsymbol{A} - \alpha \bar{\boldsymbol{A}}\right) \succeq 0 \tag{21}$$

For simplicity, the optimisation problem is a single objective, with the 10% rule as only constraint:

$$\begin{array}{ll} \min\limits_{\boldsymbol{x}} & f \\ s.t. & \boldsymbol{A} - \alpha \cdot \bar{\boldsymbol{A}} \geq 0 \end{array} \tag{22}$$

Using the Cholesky product: $\bar{\boldsymbol{A}} = \boldsymbol{L} \cdot \boldsymbol{L}^T$, $\boldsymbol{X}$ can be defined as

$$\boldsymbol{X} = \boldsymbol{L}^{-1} \cdot \boldsymbol{A} \cdot \boldsymbol{L}^{-T}, \tag{23}$$

and the constraint on positive semi-definiteness can be written as:

$$\boldsymbol{X} - \alpha \cdot \boldsymbol{I} \geq 0 \tag{24}$$

$\boldsymbol{X}$ can be approximated as:

$$\boldsymbol{X} = \boldsymbol{X}_0 + \sum_{i=1}^{L} \boldsymbol{X}_i x_i \tag{25}$$

where $\boldsymbol{X}_i$ is defined as

$$\boldsymbol{X}_i = \boldsymbol{L}^{-1} \cdot \frac{\partial \boldsymbol{A}}{\partial x_i} \cdot \boldsymbol{L}^{-T} \tag{26}$$

Adding the slack matrix $\boldsymbol{Z}$, which has to be positive semi-definite, and approximating all functions the optimisation can be written as:

$$\begin{array}{ll} \min\limits_{\boldsymbol{x}} & f(x) + \rho_1 \cdot d_1(x) \\ s.t. & \boldsymbol{X}_0 + \sum_{i=1}^{L} \boldsymbol{X}_i x_i - \alpha \cdot \boldsymbol{I} - \rho_2 \cdot d_2(x) \cdot \boldsymbol{I} - \boldsymbol{Z} = \boldsymbol{0} \\ & \boldsymbol{Z} \geq 0 \end{array} \tag{27}$$

with the damping function d_2 defined as

$$d_2 = \Delta\theta \left(\frac{1}{n_l^2} \begin{bmatrix} 1 & -1 & & & & \\ -1 & 2 & -1 & & & \\ & \ddots & \ddots & & & \\ & & -1 & 2 & -1 & \\ & & & -1 & 1 & \end{bmatrix} + \alpha \begin{pmatrix} 1 & \dots & 1 \\ \vdots & \ddots & \vdots \\ 1 & \cdots & 1 \end{pmatrix} \right) \cdot \Delta\theta \tag{28}$$

Writing the Lagrangian:

$$\mathcal{L} = f(x) + \rho_1 d_1(x) - \boldsymbol{Y} : \left(\boldsymbol{X}_0 + \sum_{i=1}^{L} \boldsymbol{X}_i x_i - \alpha \cdot \boldsymbol{I} - \rho_2 d_2(x) \cdot \boldsymbol{I} - \boldsymbol{Z} \right) - \mu ln\left(det(\boldsymbol{Z})\right) \tag{29}$$

Just as for the angle limits, the solution procedure is explained in Appendix B.

VII. Other guidelines

The guidelines that are not yet discussed do not require special constraints on the stacking sequence. Some are hard-coded in the optimisation, others are user-defined options. How each guideline can be adhered to is discussed in this section.

The following options define how the *design layers* are related to the actual lay-up:

- the symmetric constraint, rule 6, is hard-coded: every laminate is symmetric, only half the stack, the design layers are optimised, and mirrored to obtain the complete laminate.

- the balance constraint and setting the ±45°pair next to each other, rules 7 and 8, are set by the balancing option. If turned on the design layers $[\boldsymbol{\theta_1/\theta_2}]$ relate to $[\boldsymbol{\theta_1/-\theta_1/\theta_2/-\theta_2}]_S$.
- adding a fabric layer, rule 9, can be done by defining this layer in the initial guess, and removing this layer from the layers to be optimised. This means that the design layers $[\boldsymbol{\theta_1/\theta_2}]$ relate to $[\text{fabric}/\boldsymbol{\theta_1/-\theta_1/\theta_2/-\theta_2}]_S$, assuming the balancing option is turned on.
- adding the ±45 °layers on the outside, rule 10, can be done in the same way as the fabric layer: by defining the outer layer(s) and removing them from the optimisation. This means that the design layers $[\boldsymbol{\theta_1/\theta_2}]$ relate to $[\boldsymbol{45/-45/\theta_1/-\theta_1/\theta_2/-\theta_2}]_S$, assuming the balancing option is turned on.

The homogeneity rule, rule 11, which states several plies of the same orientation should be bound together is not implemented since the orientation in NCL is a continuous variable. When only four different orientations are possible, from a certain number of plies it is unavoidable to stack plies with the same direction together, however, the orientation is continuous in this work, so it can be avoided to have the same orientation next to each other. Furthermore, this rule directly contradicts the idea of dispersed laminates, rule 2.

Also rule 12, which states that a reasonable number or primary load-carrying plies should be kept away from the outer surfaces is not implemented. This has two reasons. One, the outer surface can already be defined if wanted. Two, this rule relies on engineering judgement: it cannot be formulated as a constraint. The idea behind the rule, which is improving the impact-resistance, is implemented using the dispersed and/or APPLY laminates.

VIII. Results

To check the influence of the different constraints and whether a feasible solution is found, a strength optimisation will be performed. The model is a square panel with sides of 500 mm, simply supported all around, and with the edges constrained to remain straight. The plate is loaded under bi-axial tension: N_x and N_y are used in different ratios. The material used has the following properties: $E_1 = 154$GPa, $E_2 = 10.8$GPa, $G_{12} = 4.02$GPa, $\nu_{12} = 0.317$, $t_{ply} = 0.6$mm. The laminate consists of 36 layers, and is balanced and symmetric, meaning 9 design layers are optimised.

A. Influence of the ply-count percentage rule

First only the influence of the ply-count percentage constraint, or 10% rule, is investigated: different values for the ply-count percentage are checked, with no limits on the angles. Only one ratio is checked: $N_x/N_y = 1/6$. The laminate is balanced. First, the optimisation is performed without constraint, and then it is found the laminate has a ply-count percentage of 3.67%. Next, the optimisation is repeated for values from 4 to 17 %. The factor of safety, normalised with respect to a quasi-isotropic laminate, is shown in Figure 5.

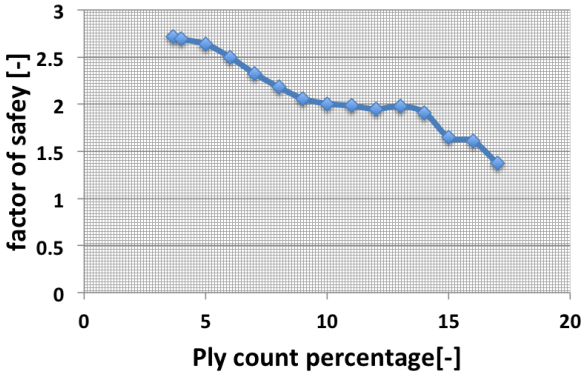

Figure 5. factor of safety for different values of the ply-count percentage

Looking at the results it can be seen that the general trend is as expected: the larger the ply-count percentage has to be, the lower the factor of safety is. An interesting point to notice is the flat piece that occurs between 10 and 13 %. There is even a small increase in factor of safety with a constraint of 13% compared to 12 %. This shows the non-convexity of the ply-count percentage constraint: the optimiser gets steered into a different local optimum by the constraints, but it turns out to be slightly better. When starting the optimisation with a constraint of 12% from the optimum for 13%, a factor of safety of 2.07 is found, which is clearly better than for 13%, and even an improvement with respect to the 9% constraint from a different starting point. This once more shows the non-convexity of the robustness rule.

Another interesting point are the steep drops for 15 and 17 %. These are most likely caused by the optimiser getting steered to a different local optimum since the direction for the optima found for lower values of the ply-count percentage constraint is no longer feasible. This shows that local optima can work both ways: one can get lucky and find a better local optimum with a higher robustness constraint, or the performance significantly decreases.

B. Influence of other design guidelines

In this optimisation, multiple ratios for N_x/N_y will be checked. All constraints described are active: the 'traditional' 10% rule is used as ply-count percentage, a minimum angle of 5°is used, a maximum angle of 85°, a minimum angle difference of 10°and a maximum angle difference of 45°.

As was shown in the previous section, the optimisation is prone to getting stuck in a local optimum. This is an inherent disadvantage of using a gradient-based optimisation. The advantage is that the optimisation is quite quick, a single run takes no longer than 30 minutes, thus multiple starting points can be checked.

The results for different ratios and different starting points are shown in Table 1. Start 1 is $[\pm 10/\pm 40/\pm 70/\pm 45/\pm 30/\pm 50/\pm 75/\pm 40/\pm 15]_s$, start 2 is $[\pm 6/\pm 17/\pm 28/\pm 39/\pm 50/\pm 61/\pm 72/\pm 63/\pm 50]_s$, and start 3 is $[\pm 30/\pm 60/\pm 30/\pm 60/\pm 30/\pm 60/\pm 30/\pm 60/\pm 30]_s$. The results show the factor of safety, normalised with respect to the factor of safety of a quasi-isotropic laminate. Normalisation is always done with respect to the factor of safety for the specific loading condition. The constraints are satisfied for each case.

Table 1. Factor of safety normalised with respect to the quasi-isotropic factor of safety for different ratios of N_y/N_x

ratio	start 1	start 2	start 3
0	1.522	1.156	1.266
0.25	1.870	1.815	1.431
0.5	1.543	1.638	1.635
0.75	1.222	0.999	1.220
1	0.995	0.995	0.999

Looking at the results in Table 1 it can be noticed that the factor of safety does not always increase to the same point, showing again that the optimisation is prone to getting stuck in a local optimum. However, except for a ratio of 0, meaning uni-axial loading in x-direction, the highest two values are close together. It can also be seen that, fro a ratio of 0.25 onward, the normalised factor of safety is always increasing, indicating that the laminate is getting closer to the behaviour of a quasi-isotropic laminate. This is expected since the closer the ratio of N_y/N_x gets to one, the closer the ideal stiffness E_y/E_x gets to one, and thus the closer the laminate gets to quasi-isotropic behaviour.

For a ratio of 1, the theoretical optimum is a quasi-isotropic laminate, and this is almost what was found. At least, the behaviour of the laminate is like a quasi-isotropic one: the lay-up for the three optima is very different. From start 1, the optimum found is $[\pm 13/\pm 34/\pm 69/\pm 48/\pm 31/\pm 58/\pm 79/\pm 51/\pm 21]_s$, from start 2 $[\pm 8/\pm 20/\pm 30/\pm 40/\pm 50/\pm 66/\pm 83/\pm 65/\pm 42]_s$, and from start 3 $[\pm 28/\pm 59/\pm 32/\pm 60/\pm 31/\pm 63/\pm 34/\pm 67/\pm 33]_s$. This shows one of the reasons for the presence of local optima: different lay-ups lead to (almost) the same factor of safety.

IX. Conclusion

In this paper a method to pose design guidelines as constraints in a gradient-based optimisation is described. Different rules concerning limits on angles and angle difference were implemented. The ply-count percentage, the 'traditional' 10% rule, was interpreted as a limit on the ratio between the minimum and maximum stiffness. This was then implemented as a positive semi-definite matrix constraint. Convex approximations of the structural responses are made in terms of the fibre angles. The method of successive approximations was used in combination with a predictor-corrector interior-point method to perform the optimisation.

Initial results indicate that the method does adhere to all constraints posed, and satisfying results are obtained. A square plate simply supported all around under bi-axial tension is optimised to improve the factor of safety. The influence of the ply-count percentage was checked for a fixed value of the ratio between N_x and N_y. Results were as expected: the higher the robustness, the lower the factor of safety. However, it was observed sometimes the optimisation got stuck in a local optimum. Hence, for the second case, where multiple multiple ratios of N_y/N_x were used, initial guesses were used, and all constraints were active. This optimisation confirmed that the constraints were satisfied in each case, but the results were dependent of the initial guess.

The results showed the importance of having the design guidelines implemented. Multiple laminates having (almost) the same performance, but different lay-up were identified, all obeying the design guidelines. This shows the reason for the multiple local optima: lay-ups that look completely different at first sight may have the same structural behaviour. While from an optimisation point-of-view these multiple optima are hard to handle, they may have benefits as well: other considerations can determine which of the lay-ups is best suited at a certain location. Hence, these multiple optima give the user a set of possible lay-ups, which he can judge from a different perspective, without having to worry about structural performance.

X. Acknowledgements

This work is supported by the CANAL (CreAting Non-conventionAl Laminates) Project, part of the European Union Seventh Framework Program.

Appendix A: solution procedure for the angle limits

Starting from the Lagrangian, equation 13, the optimality conditions are found to be:

$$-r_{x_j} = \boldsymbol{g} + \rho_1 \cdot \boldsymbol{g}^{(1)} + \sum_k \lambda_k \cdot \left(sin\left(2\theta_k - 2\theta_{k+1}\right) \cdot \frac{\partial\left(\theta_k - \theta_{k+1}\right)}{\partial \theta_j} + \rho_3 \cdot \boldsymbol{g}^{(3)} \right) \tag{30}$$

$$-r_{\lambda_k} = sin\left(\theta_k - \theta_{k+1}\right)^2 - M + \rho_3 \cdot d_{(3k)}(x) + s_{d_k} \tag{31}$$

$$-r_{s_{d_k}} = \lambda_k \cdot s_{d_k} - \mu \tag{32}$$

Linearising:

$$\begin{aligned} r_{x_j} = \quad & \boldsymbol{H} \cdot \boldsymbol{dx} + \rho_1 \boldsymbol{H^{(1)}} \cdot \boldsymbol{dx} + \textstyle\sum_k \lambda_k \cdot 2 \cdot cos(2\theta_k - 2\theta_{k+1}) \cdot \left(\frac{\partial(\theta_k - \theta_{k+1})}{\partial \theta_j} \right)^2 \cdot dx_j + \\ & + \lambda_k \rho_3 \boldsymbol{H^{(3)}} \cdot \boldsymbol{dx} + \boldsymbol{d\lambda} \cdot \left(sin\left(2\theta_k - 2\theta_{k+1}\right) \cdot \frac{\partial(\theta_k - \theta_{k+1})}{\partial \theta_j} + \rho_3 \cdot \boldsymbol{g}^{(3k)} \right) \\ r_{\lambda_k} = \quad & \textstyle\sum_j sin\left(2\theta_k - 2\theta_{k+1}\right) \cdot \frac{\partial(\theta_k - \theta_{k+1})}{\partial \theta_j} dx_j + \rho_3 \cdot \boldsymbol{g}^{(3k)} \cdot \boldsymbol{dx} + ds_{d_k} \\ r_{s_d} = \quad & d\lambda_k \cdot s_{d_k} + \lambda \cdot ds_{d_k} \end{aligned} \tag{33}$$

To shorten the notation, define row k of $\boldsymbol{G}_t$ as

$$\boldsymbol{g}_{t,k} = \rho_3 \cdot \boldsymbol{g}^{(3k)} + \boldsymbol{dg(k)} \tag{34}$$

with $\boldsymbol{dg(k)}$ defined as

$$dg(k)_j = sin\left(2\theta_k - 2\theta_{k+1}\right) \cdot \frac{\partial\left(\theta_k - \theta_{k+1}\right)}{\partial \theta_j} \tag{35}$$

Furthermore, defining $\boldsymbol{H_i}$ as:

$$\boldsymbol{H_i} = \boldsymbol{H} + \rho_1 \boldsymbol{H^{(1)}} + \boldsymbol{H^{(4)}} + \lambda_k \rho_3 \boldsymbol{H^{(3)}} \tag{36}$$

with the j-th row of $\boldsymbol{H^{(4)}}$ defined as:

$$\boldsymbol{H^{(4)}} = \sum_k \lambda_k \cdot 2 \cdot cos(2\theta_k - 2\theta_{k+1}) \cdot \left(\frac{\partial \left(\theta_k - \theta_{k+1}\right)}{\partial \theta_j} \right)^2 \tag{37}$$

To guarantee that the approximation is convex, the terms in $\boldsymbol{H^{(4)}}$ need to be positive. If this is not the case, the term is set to zero.

Defining $\boldsymbol{\lambda}$ and $\boldsymbol{S_d}$ as the diagonal matrices containing λ_k and S_{d_k} on their diagonal, the linearisation can be rewritten as:

$$\begin{aligned} r_x = &\quad \boldsymbol{H_i} \cdot \boldsymbol{dx} + \boldsymbol{G_t}^T \boldsymbol{d\lambda} \\ r_\lambda = &\quad \boldsymbol{G_t} \cdot \boldsymbol{dx} + \boldsymbol{dS_d} \\ r_{S_d} = &\quad \boldsymbol{d\lambda} \cdot \boldsymbol{S_d} + \boldsymbol{\lambda} \cdot \boldsymbol{dS_d} \end{aligned} \tag{38}$$

From these, $\boldsymbol{dS_d}$ and $\boldsymbol{d\lambda}$ can be found to be:

$$\boldsymbol{d\lambda} = \boldsymbol{S_d}^{-1} \cdot (\boldsymbol{r_{s_d}} - \boldsymbol{\lambda} \boldsymbol{dS_d}) \tag{39}$$

$$\boldsymbol{dS_d} = \boldsymbol{r_\lambda} - \boldsymbol{G_t dx} \tag{40}$$

Filling this into the equation for r_x leads to:

$$r_x = \boldsymbol{H_i} \cdot \boldsymbol{dx} + \boldsymbol{G_t}^T \cdot \boldsymbol{S_d}^{-1} \cdot (\boldsymbol{r_{s_d}} - \boldsymbol{\lambda} (\boldsymbol{r_\lambda} - \boldsymbol{G_t dx})) \tag{41}$$

Rewriting leads to:

$$r_x - \boldsymbol{G_t}^T \cdot \boldsymbol{S_d}^{-1} \cdot \boldsymbol{r_{s_d}} + \boldsymbol{G_t}^T \cdot \boldsymbol{S_d}^{-1} \cdot \boldsymbol{\lambda} \cdot \boldsymbol{r_\lambda} = \left(\boldsymbol{H_i} + \boldsymbol{G_t}^T \cdot \boldsymbol{S_d}^{-1} \cdot \boldsymbol{\lambda} \cdot \boldsymbol{G_t} \right) \cdot \boldsymbol{dx} \tag{42}$$

Hence, only the expression for r_x and the Hessian are changed. The same holds for the minimal difference between adjacent plies and the limits on angles themselves: they will have a similar form. Also the $sin(\theta)^2$ form will be used in these cases.

For the other three differences, the constraint can be written as:

$$\begin{array}{ccc} \text{minimal angle difference} & sin\left(\theta_k - \theta_{k+1}\right)^2 \geq m & k = 1, ..., l-1 \\ \text{maximal angle} & sin\left(\theta_k\right)^2 \leq D & k = 1, ..., l \\ \text{minimal angle} & sin\left(\theta_k\right)^2 \geq d & k = 1, ..., l \end{array} \tag{43}$$

The change in G is only due to a different $dg(k)$, defined in equation 35 for the maximal angle change. This has to be defined as follows for the different constraints:

$$\begin{array}{cc} \text{minimal angle difference} & dg(k)_j = -sin\left(2\theta_k - 2\theta_{k+1}\right) \cdot \frac{\partial(\theta_k - \theta_{k+1})}{\partial \theta_j} \\ \text{maximal angle} & dg(k)_j = sin(2\theta_k) \frac{\partial \theta_k}{\partial \theta_j} \\ \text{minimal angle} & dg(k)_j = -sin(2\theta_k) \frac{\partial \theta_k}{\partial \theta_j} \end{array} \tag{44}$$

The Hessian changes only due to a change in $\boldsymbol{H}^{(4)}$, defined in equation 37 for the maximal angle change. This has to be defined as follows for the different constraints:

$$\begin{array}{cc} \text{minimal angle difference} & \boldsymbol{H^{(4)}} = -\sum_k \lambda_k \cdot 2 \cdot cos(2\theta_k - 2\theta_{k+1}) \cdot \left(\frac{\partial(\theta_k - \theta_{k+1})}{\partial \theta_j} \right)^2 \\ \text{maximal angle} & \boldsymbol{H^{(4)}} = \sum_k \lambda_k \cdot 2 \cdot cos(2\theta_k) \cdot \left(\frac{\partial \theta_k}{\partial \theta_j} \right)^2 \\ \text{minimal angle} & \boldsymbol{H^{(4)}} = -\sum_k \lambda_k \cdot 2 \cdot cos(2\theta_k) \cdot \left(\frac{\partial \theta_k}{\partial \theta_j} \right)^2 \end{array} \tag{45}$$

Furthermore, the damping function for the limits on angles is changed to:

$$d_4 = \frac{\left(\Delta \theta_k\right)^2}{2} \tag{46}$$

Appendix B: solution procedure for the angle limits

Starting from the Lagrangian for this problem, equation 29, first the matrices are rewritten. Instead of the 2-dimensional arrays $\boldsymbol{X}_i$, one can also define a 3-dimensional array $\boldsymbol{\mathcal{X}}$, such that $\boldsymbol{\mathcal{X}}_{abi} = \boldsymbol{X}_i$. Defining two operators:

$$\boldsymbol{\mathcal{X}}^T \cdot \boldsymbol{Y} = \sum_{i=1}^{L} \boldsymbol{\mathcal{X}}_{abi} \cdot \boldsymbol{Y}_{ab} \tag{47}$$

$$\boldsymbol{\mathcal{X}} \cdot \boldsymbol{x} = \sum_{i=1}^{L} \boldsymbol{\mathcal{X}}_{abi} \cdot \boldsymbol{x}_i \tag{48}$$

The optimality conditions are found to be:

$$\begin{array}{rc} -r_x = & \boldsymbol{g} + \rho_1 \boldsymbol{g}^{(1)} - \boldsymbol{\mathcal{X}}^T \cdot \boldsymbol{Y} + \rho_2 \left(\boldsymbol{Y} : \boldsymbol{I}\right) \boldsymbol{g}^{(2)} \\ -r_{\boldsymbol{Y}} = & -\boldsymbol{X}_0 - \boldsymbol{\mathcal{X}}^T \cdot \boldsymbol{x} + \alpha \cdot \boldsymbol{I} + \rho_2 d_2(x) \cdot \boldsymbol{I} + \boldsymbol{Z} \\ -r_{\boldsymbol{Z}} = & \boldsymbol{Z} \cdot \boldsymbol{Y} - \mu \cdot \boldsymbol{I} \end{array} \tag{49}$$

Linearising leads to

$$\begin{array}{rc} r_x = & \boldsymbol{H} \cdot \boldsymbol{dx} + \rho_1 \boldsymbol{H^{(1)}} \cdot \boldsymbol{dx} + \rho_2 \left(\boldsymbol{Y} : \boldsymbol{I}\right) \cdot \boldsymbol{H^{(2)}} \cdot \boldsymbol{dx} - \boldsymbol{\mathcal{X}}^T \cdot \boldsymbol{dY} + \rho_2 \left(\boldsymbol{dY} : \boldsymbol{I}\right) \cdot \boldsymbol{g}^{(2)} \\ r_{\boldsymbol{Y}} = & -\boldsymbol{\mathcal{X}} \cdot \boldsymbol{dx} + \rho_2 \left(\boldsymbol{g}^{(2)T} \cdot \boldsymbol{dx}\right) \cdot \boldsymbol{I} + \boldsymbol{dZ} \\ r_{\boldsymbol{Z}} = & \boldsymbol{dZ} \cdot \boldsymbol{Y} + \boldsymbol{Z} \cdot \boldsymbol{dY} \end{array} \tag{50}$$

Defining $\boldsymbol{H^{(5)}}$ as:

$$\boldsymbol{H^{(5)}} = \boldsymbol{H} + \rho_1 \cdot \boldsymbol{H}^{(1)} + \rho_2 \cdot \left(\boldsymbol{Y} : \boldsymbol{I}\right) \boldsymbol{H}^{(2)} \tag{51}$$

From the linearised equations for $r_{\boldsymbol{Y}}$ and $r_{\boldsymbol{Z}}$, it can be found that:

$$\begin{array}{c} \boldsymbol{dZ} = r_{\boldsymbol{Y}} + \boldsymbol{\mathcal{X}} \cdot \boldsymbol{dx} - \rho_2 \left(\boldsymbol{g}^{(2)T} \cdot \boldsymbol{dx}\right) \cdot \boldsymbol{I} \\ \boldsymbol{dY} = \boldsymbol{Z}^{-1} \cdot r_{\boldsymbol{z}} - \boldsymbol{Z}^{-1} \cdot \boldsymbol{dZ} \cdot \boldsymbol{Y} \end{array} \tag{52}$$

Substituting these expressions gives:

$$\begin{array}{c} r_x = \boldsymbol{H^{(5)}} \boldsymbol{dx} + \rho_2 \left(\left(\boldsymbol{Z}^{-1} \boldsymbol{r_z} - \boldsymbol{Z}^{-1} \left(\boldsymbol{r_y} + \left(\boldsymbol{\mathcal{X}} \cdot \boldsymbol{dx}\right) - \rho_2 \left(\boldsymbol{g}^{(2)T} \boldsymbol{dx}\right) \boldsymbol{I}\right) \boldsymbol{Y}\right) : \boldsymbol{I}\right) \boldsymbol{g}^{(2)} - \\ \boldsymbol{\mathcal{X}}^T \cdot \left(\boldsymbol{Z}^{-1} \boldsymbol{r_z} - \boldsymbol{Z}^{-1} \left(\boldsymbol{r_y} + \boldsymbol{\mathcal{X}} \cdot \boldsymbol{dx} - \rho_2 \left(\boldsymbol{g}^{(2)T} \boldsymbol{dx}\right) \boldsymbol{I}\right) \boldsymbol{Y}\right) \end{array} \tag{53}$$

rewriting:

$$\begin{array}{c} r_x^* = r_x - \rho_2 \left(\left(\boldsymbol{Z}^{-1} \boldsymbol{r_z} - \boldsymbol{Z}^{-1} \boldsymbol{r_y} \boldsymbol{Y}\right) : \boldsymbol{I}\right) \boldsymbol{g}^{(2)} + \boldsymbol{\mathcal{X}}^T \cdot \left(\boldsymbol{Z}^{-1} \boldsymbol{r_z} - \boldsymbol{Z}^{-1} \boldsymbol{r_y} \boldsymbol{Y}\right) = \\ \boldsymbol{H^{(5)}} \boldsymbol{dx} - \rho_2 \left(\left(\boldsymbol{Z}^{-1} \left(\boldsymbol{\mathcal{X}} \cdot \boldsymbol{dx}\right) \boldsymbol{Y}\right) : \boldsymbol{I}\right) \boldsymbol{g}^{(2)} + \rho_2^2 \left(\boldsymbol{Z}^{-1} \left(\boldsymbol{g}^{(2)T}\right) \boldsymbol{dx} \boldsymbol{I} \boldsymbol{Y} : \boldsymbol{I}\right) \boldsymbol{g}^{(2)} + \\ \boldsymbol{\mathcal{X}}^T \boldsymbol{Z}^{-1} \left(\boldsymbol{\mathcal{X}} \cdot \boldsymbol{dx}\right) \boldsymbol{Y} - \rho_2 \boldsymbol{\mathcal{X}}^T \boldsymbol{Z}^{-1} \left(\boldsymbol{g}^{(2)T} \boldsymbol{dx}\right) \boldsymbol{I} \boldsymbol{Y} \end{array} \tag{54}$$

This needs to be rewritten in the form $\boldsymbol{V} \cdot \boldsymbol{dx}$, for all parts:

$$\boldsymbol{\mathcal{X}}^T \boldsymbol{Z}^{-1} \left(\boldsymbol{\mathcal{X}} \cdot \boldsymbol{dx}\right) \boldsymbol{Y} = \boldsymbol{\mathcal{X}}^T \boldsymbol{Z}^{-1} \boldsymbol{\mathcal{X}}^T \cdot \boldsymbol{Y} \cdot \boldsymbol{dx} = \boldsymbol{H^{(6)}} \cdot \boldsymbol{dx} \tag{55}$$

To program it in a matrix environment, the 3-dimensional arrays are not defined, hence one has to use:

$$\boldsymbol{H^{(6)}}_{ij} = \left[\boldsymbol{\mathcal{X}}^T \boldsymbol{Z}^{-1} \boldsymbol{\mathcal{X}}^T \cdot \boldsymbol{Y}\right]_{ij} = \left(\boldsymbol{X_i} \cdot \boldsymbol{Z}^{-1} \cdot \boldsymbol{X_j}\right) : \boldsymbol{Y} \tag{56}$$

The other parts can be written as (sum of) 2-dimensional arrays:

$$\begin{array}{c} \boldsymbol{\mathcal{X}}^T \boldsymbol{Z}^{-1} \left(\boldsymbol{g}^{(2)T} \boldsymbol{dx}\right) \boldsymbol{I} \boldsymbol{Y} = \boldsymbol{\mathcal{X}}^T \boldsymbol{Z}^{-1} \boldsymbol{Y} \cdot \boldsymbol{g}^{(2)T} \boldsymbol{dx} = \sum_i \boldsymbol{X_i}^T \boldsymbol{Z}^{-1} \boldsymbol{Y} \cdot \boldsymbol{g}^{(2)T} dx_i = \boldsymbol{b}^{(2)} \boldsymbol{g}^{(2)} \boldsymbol{dx} \\ \left(\boldsymbol{Z}^{-1} \left(\boldsymbol{\mathcal{X}} \cdot \boldsymbol{dx}\right) \boldsymbol{Y} : \boldsymbol{I}\right) \boldsymbol{g}^{(2)} = tr\left(\boldsymbol{Z}^{-1} \left(\boldsymbol{\mathcal{X}} \cdot \boldsymbol{dx}\right) \boldsymbol{Y}\right) \boldsymbol{g}^{(2)} = \sum_i tr\left(\boldsymbol{Z}^{-1} \boldsymbol{X_i} \boldsymbol{Y}\right) \boldsymbol{g}^{(2)} dx_i = \boldsymbol{b}^{(1)} \boldsymbol{g}^{(2)} \boldsymbol{dx} \\ \left(\boldsymbol{Z}^{-1} \left(\boldsymbol{g}^{(2)T} \boldsymbol{dx}\right) \boldsymbol{I} \boldsymbol{Y} : \boldsymbol{I}\right) \boldsymbol{g}^{(2)} = tr\left(\boldsymbol{Z}^{-1} \left(\boldsymbol{g}^{(2)T} \boldsymbol{dx}\right) \boldsymbol{I} \boldsymbol{Y}\right) \boldsymbol{g}^{(2)} = tr\left(\boldsymbol{Z}^{-1} \boldsymbol{Y}\right) \boldsymbol{g}^{(2)} \boldsymbol{g}^{(2)T} \boldsymbol{dx} = \boldsymbol{H^{(7)}} \boldsymbol{dx} \end{array} \tag{57}$$

with:

$$\begin{aligned} \boldsymbol{b} &= tr\left(\boldsymbol{Z}^{-1}\boldsymbol{X_i}\boldsymbol{Y}\right) \\ \boldsymbol{H^{(7)}} &= tr\left(\boldsymbol{Z}^{-1}\boldsymbol{Y}\right)\boldsymbol{g}^{(2)}\boldsymbol{g}^{(2)T} \end{aligned} \tag{58}$$

Hence, in $r_x^* = \boldsymbol{V} \cdot \boldsymbol{dx}$, $\boldsymbol{V}$ is given by:

$$\boldsymbol{V} = \boldsymbol{H} + \rho_1 \cdot \boldsymbol{H}^{(1)} + \rho_2 \cdot (\boldsymbol{Y} : \boldsymbol{I})\, \boldsymbol{H}^{(2)} + \boldsymbol{H^{(6)}} + \rho_2^2 \boldsymbol{H^{(7)}} - \rho_2 \cdot \boldsymbol{g}^{(2)} \cdot \boldsymbol{b}^T - \rho_2 \cdot \boldsymbol{b} \cdot \boldsymbol{g}^{(2)T} \tag{59}$$

Hence, analogue to the angle limits, only the expression for r_x and the Hessian change. This implies all rules can be set at the same time, by combining the changes in r_x and the Hessian.

To determine the primal step size, the slack $\boldsymbol{Z}$ should stay positive semi-definite; to determine the dual step size, the dual variable $\boldsymbol{Y}$ should stay positive semi-definite. Using

$$(\boldsymbol{Z} + \eta \boldsymbol{dZ})\, \boldsymbol{a} = \boldsymbol{0} \tag{60}$$

the maximum step size is the smallest negative eigenvalue.

References

[1]Kassapoglou, C., *Design and analysis of composite structures*, John Wiley and Sons, Ltd, 2010.

[2]"Boeing 787 from the gound up," `http://www.boeing.com/commercial/aeromagazine/articles/qtr_4_06/AERO_Q406_article4.pdf`, Accessed: 10 November 2015.

[3]"A350XWB Technology," `http://www.airbus.com/aircraftfamilies/passengeraircraft/a350xwbfamily/technology-and-innovation`, Accessed: 10 November 2015.

[4]Ghiasi, H., Pasini, D., and Lessard, L., "Optimum stacking sequence design of composite materials Part I: Constant stiffness design," *Composite Structures*, Vol. 90, No. 1, 2009, pp. 1 – 11.

[5]Honda, S., Narita, Y., and Sasaki, K., "Discrete Optimization for Vibration Design of Composite Plates by Using Lamination Parameters," *Advanced Composite Materials*, Vol. 18, No. 4, 2009, pp. 297–314.

[6]Liu, S., Hou, Y., Sun, X., and Zhang, Y., "A two-step optimization scheme for maximum stiffness design of laminated plates based on lamination parameters," *Composite Structures*, Vol. 94, No. 12, 2012, pp. 3529 – 3537.

[7]Raju, G., White, S., Wu, Z., and Weaver, P., *Optimal Postbuckling Design of Variable Angle Tow Composites using Lamination Parameters*, American Institute of Aeronautics and Astronautics, 2015/03/30 2015.

[8]LE RICHE, R. and HAFTKA, R. T., "Optimization of laminate stacking sequence for buckling load maximization by genetic algorithm," *AIAA Journal*, Vol. 31, No. 5, 2015/05/18 1993, pp. 951–956.

[9]Aymerich, F. and Serra, M., "Optimization of laminate stacking sequence for maximum buckling load using the ant colony optimization (ACO) metaheuristic," *Composites Part A: Applied Science and Manufacturing*, Vol. 39, No. 2, 2008, pp. 262 – 272.

[10]Fleury, C., "CONLIN: An efficient dual optimizer based on convex approximation concepts," *Structural optimization*, Vol. 1, No. 2, 1989, pp. 81–89.

[11]Svanberg, K., "a class of globally convergent optimization methods based on conservative convex separable approximations," *Siam J. optim*, Vol. 2, 2002, pp. 555–573.

[12]Peeters, D. M., Hesse, S., and Abdalla, M. M., "Stacking sequence optimisation of variable stiffness laminates with manufacturing constraints," *Composite Structures*, Vol. 125, No. 0, 2015, pp. 596 – 604.

[13]Grunenfelder, L., Suksangpanya, N., Salinas, C., Milliron, G., Yaraghi, N., Herrera, S., Evans-Lutterodt, K., Nutt, S., Zavattieri, P., and Kisailus, D., "Bio-inspired impact-resistant composites," *Acta Biomaterialia*, Vol. 10, No. 9, 2014, pp. 3997 – 4008, Biomineralization.

[14]Lopes, C., Seresta, O., Abdalla, M., Gurdal, Z., Thuis, B., and Camanho, P., *Stacking Sequence Dispersion and Tow-Placement for Improved Damage Tolerance*, American Institute of Aeronautics and Astronautics, 2015/05/26 2008.

[15]Lopes, C., Camanho, P., Gürdal, Z., Maim, P., and Gonzlez, E., "Low-velocity impact damage on dispersed stacking sequence laminates. Part II: Numerical simulations," *Composites Science and Technology*, Vol. 69, No. 78, 2009, pp. 937 – 947.

[16]Sebaey, T., Gonzlez, E., Lopes, C., Blanco, N., and Costa, J., "Damage resistance and damage tolerance of dispersed {CFRP} laminates: Design and optimization," *Composite Structures*, Vol. 95, No. 0, 2013, pp. 569 – 576.

[17]Nagelsmit, M., Kassapoglou, C., and Gürdal, Z., "AP-PLY: A New Fibre Placement Architecture for Fabric Replacement," *SAMPE Journal*, Vol. 47, No. 2, 2011, pp. 36 – 45.

[18]Beckwith, S. W., "Designing with Composites: Suggested Best Practices Rules," *SAMPE journal*, Vol. 45, 2009, pp. 36 – 37.

[19]Bailie, J., Ley, R., and Pasricha, A., "A summary and review of composite laminate design guidelines," *Langley RC, Hampton*, 1997.

[20]de Wit, A. and van Keulen, F., "Numerical Comparison of Multi-Level Optimization Techniques," *48th AIAA/ASME/ASCE/AHS/ASC Structures, Structural Dynamics, and Materials Conference*, American Institute of Aeronautics and Astronautics, 2014/11/11 2007.

[21]IJsselmuiden, S. T., *Optimal design of variable stffness composite structures using lamination parameters*, Ph.D. thesis, Delft University of Technology, 2011.

[22]Haftka, R. and Gürdal, Z., *Elements of Structural Optimization*, Contributions to Phenomenology, Springer Netherlands, 1992.

[23]Kumar, V., Lee, S.-J., and German, M., "Finite element design sensitivity analysis and its integration with numerical optimization techniques for structural design," *Computers and Structures*, Vol. 32, No. 34, 1989, pp. 883 – 897.

[24]Herakovich, C. T., "On the relationship between engineering properties and delamination of composite materials," *Journal of Composite Materials*, Vol. 15, 1981, pp. 336–348.

[25]Abdalla, M. M., Kassapoglou, C., and Gürdal, Z., "an invariant robustness rule for composite design," *composite science and technology*, submitted.

[26]Irisarri, F.-X., Lasseigne, A., Leroy, F.-H., and Riche, R. L., "Optimal design of laminated composite structures with ply drops using stacking sequence tables," *Composite Structures*, Vol. 107, No. 0, 2014, pp. 559 – 569.